AAPS PharmSciTech, Vol. 13, No. 2, June 2012 (© 2012)
DOI: 10.1208/s12249-012-9768-5

Research Article

Physicochemical Performances of Indomethacin in Cholesteryl Cetyl Carbonate Liquid Crystal as a Transdermal Dosage

Nunchanit Aeinleng,[1] Sarunyou Songkro,[1,2] Kusumarn Noipha,[1,3] and Teerapol Srichana[1,2,4]

Received 13 May 2011; accepted 28 February 2012; published online 20 March 2012

Abstract. A transdermal formulation of indomethacin (IMC) was developed by incorporation into cholesteryl cetyl carbonate (CCC). The liquid crystalline phase properties of the IMC–CCC mixture were detected by polarized light microscopy and differential scanning calorimetry. A low drug loading was obtained (1–5 %) similar to that used in conventional topical IMC in a clinical setting. A controlled release of IMC was found over 12 h. A low amount of IMC in 1 % IMC–CCC permeated the stratum corneum. Further formulation development has been carried out by the addition of lauryl alcohol into 5 % IMC–CCC mixture it was found that the permeation of IMC was significantly improved to 45 % within 24 h.

KEY WORDS: permeation; skin; transdermal.

INTRODUCTION

Indomethacin (IMC) is a non-steroidal anti-inflammatory drug that reduces fever, pain and inflammation (1,2). The most common side effect of IMC is gastrointestinal irritation. IMC may cause or worsen stomach ulcers or intestinal bleeding. In severe situations, it may lead to perforation of the intestine (3,4).

IMC is practically insoluble in water (5) with a partition-coefficient in octanol/water of 3.95 (6). Numerous efforts have been made to modify the drug dissolution rate (7–10). In aqueous solutions, IMC is degraded and its therapeutic activity is impaired. Various methods have been employed to enhance the drug stability in aqueous solvent systems such as by encapsulation in liposomal suspensions, complexation of the drug with various cyclodextrins (11), entrapment into multilamellar liposomes (12), the synthesis of an ester prodrug (13) and using spray-dried nanocapsules and nanospheres (14).

In view of these problems, it is important to devise strategies to tackle them. Transdermal formulations may be another solution for improving IMC biovailability. A transdermal preparation must not only have an ability to facilitate the penetration of the drug into a painful area, but must also be devoid of any negative cutaneous reaction and must also be easy to apply. However, facilitating the cutaneous absorption of IMC is not sufficient because its release from such formulations may be limited (15), together with its ease of hydrolysis and lack of stability (12).

Several types of IMC formulations have been investigated. For instance, IMC was incorporated into a microemulsion that controlled its release (16). Phosphatidylcholine was used as a permeation enhancer of IMC (17). A liquid crystalline gel was used to control release of the IMC sodium salt, only 19 % was obtained in 24 h (15). In the cosmetic and chemical industries there have been interests in forming liquid crystalline phases for delivery systems (18) and this is now being exploited in the field of pharmacy (19). This is because such phases are thermodynamically stable, and materials can be stored for long periods of time without phase separation. Therefore, the development of liquid crystals as an aid for drug delivery systems is expected to increase the efficiency of the drug by increasing its stability and absorption (20). Liquid crystals may serve as a thermoresponsive membrane to control drug release (21,22). The liquid crystal materials used in topical/transdermal formulations are those such as cholesteryl oleyl carbonate (21) and glyceryl monooleate (19). In this study, we employed CCC (a cholesterol derivative) as an excipient for a transdermal formulation. According to the chemical properties of cholesteryl cetyl carbonate (CCC), it is a thermoresponsive material (23,24). If a drug can be incorporated into its normal cubic phase then encapsulated IMC may improve its stability. The CCC should also enhance the ability of IMC to cross the stratum corneum. In addition, such a thermotropic liquid crystal may protect the drug molecule from light. The aim of this study was to prepare IMC in an effective transdermal preparation. It is expected that such a formulation would improve IMC stability, allow for a suitable release process and enhance its ability to permeate the skin barrier.

[1] Drug Delivery System Excellence Center, Prince of Songkla University, Hat Yai, Songkla 90112, Thailand.
[2] Department of Pharmaceutical Technology, Faculty of Pharmaceutical Sciences, Prince of Songkla University, Hat Yai, Songkla 90112, Thailand.
[3] Faculty of Health and Sports Science, Thaksin University, Phatthalung 93110, Thailand.
[4] To whom correspondence should be addressed. (e-mail: teerapol.s@psu.ac.th)

MATERIALS AND METHODS

Materials

IMC was obtained from Sigma-Aldrich, St. Louis, USA. It is white odorless compound. CCC was obtained from our synthesis in house according to the method described elsewhere (25). Lauryl alcohol (LA) was supplied by Aldrich, Steinheim, Germany. Other solvent and chemicals are all analytical grade.

Methods

Solubility Study of Indomethacin in Isotonic Phosphate Buffer pH 7.4

An excess amount of IMC (10 mg) was added to isotonic phosphate buffer (IPB) pH 7.4 (10 mL) maintained at 37 °C within a shaking water bath (American Heto Lab, Maryland, USA). Then, 2-mL aliquots of the solution were removed at 24, 48, 72 h and after 72 h every hour for 3 h. Each sample was centrifuged at 10,000 rpm for 10 min. One milliliter of each supernatant was then diluted with IPB pH 7.4 to an appropriate concentration. The concentration of IMC was determined by HPLC. Solubility studies were performed in triplicate.

Chromatographic Conditions

Chromatographic separation was conducted using the high-performance liquid chromatography (HPLC) apparatus (Thermoelectron Corporation, Massachusetts, USA) on a 10 μm size, 4.6 mm×250 mm Phenomenex® RP18 stainless steel analytical column (CA, USA) fitted with a Phenomenex® security guard (CA, USA), 4 mm×20 mm C18. The mobile elution phase was 0.2 mM acetate buffer pH 5.5 and acetonitrile at a ratio of 65:35 (*v*/*v*) (6). The flow rate was 1.0 mL/min with a sample injection volume of 20 μL. The detection wavelength of IMC was 254 nm. The system was validated for its limit of quantification (LOQ) for indomethacin in IPB pH 7.4, methanol and supernatant from a skin homogenate.

Preparation of the Indomethacin–CCC (IMC–CCC) and IMC–CCC–LA Mixture

A binary mixture of various weight ratios of IMC/CCC were prepared (1:99, 2:98, and 5:95 % *w*/*w*) by dissolving 0.5 g of each ratio in 10 mL of chloroform. When the mixture was completely dissolved, the solvent was removed by a rotary evaporator. A binary mixture of CCC/LA (1:4 weight ratio) was prepared by melting CCC (1 g) and LA (4 g) at 50 °C following by the addition of IMC into the mixture for 5 % IMC loading until a homogenous mixture was obtained. The IMC–CCC mixtures were kept in a dessicator (25 °C, 46 % relative humidity) before subjecting them to thermal analysis. Samples were analyzed by a Fourier transform infrared spectrophotometer (FTIR) and differential scanning calorimetry (DSC). Each mixture was examined by sampling 10 mg from each (n=3). The sampling mixture was dissolved, adjusted to the required volume with methanol and sonicated for 10 min to obtain a clear solution. The IMC content was then determined by HPLC. Further investigation of IMC–CCC or IMC–CCC–LA mixtures was carried out by polarized light microscopy (PLM), release kinetics, and permeation across excised newborn pig skin. As each of these preparations gave homogeneous mixtures, they were suitable formulations for the permeation studies.

Fourier Transformed Infrared Spectrophotometer

The functional groups of the liquid crystal were characterized by FTIR (Spectrum one, Perkin Elmer, MA, USA) in the region 4,000–400 cm^{-1}. FTIR spectra were obtained at a 4 cm^{-1} resolution under a dry air purge, and an accumulation of eight scans. A small amount of sample was sealed into a KBr pellet by a hydraulic press prior to being measured at ambient temperature.

Differential Scanning Calorimetry

DSC (Perkin Elmer DSC 7, Massachusetts, USA) was used to investigate the thermal properties of the IMC–CCC and IMC–CCC–LA mixtures. The sample (5 mg) was placed in an aluminum pan, sealed hermetically, and then assessed by DSC in the heating mode from 20 to 200 °C followed by cooling from 200 to 20 °C at a rate of 10 °C/min. All samples were analyzed in triplicate. The DSC thermograms were analyzed using the Universal analysis 2000 program version 3.4c (TA instruments, New Castle, USA) (26).

Polarized Light Microscopy

The IMC–CCC mixtures and IMC–CCC–LA were examined with a polarized light microscope (Olympus BH-2, Japan) with a hot stage, in order to study the texture of the anisotropic phases. The sample (5 mg) was placed on a glass slide and covered with a glass cover slip (27). The IMC and CCC were examined in parallel.

The existence of a birefringence was verified by observation under the crossed polarizer at a magnification of ×400. Photographs of these samples were taken at room temperature (RT) before heating to 200 °C and after cooling down to RT. The thermal phase transitions and texture changes of the IMC–CCC mixtures were observed with an Olympus BH-2 polarizing optical microscope equipped with a hot stage (Westler, Germany).

Dissolution Test of IMC–CCC Mixtures and IMC–CCC–LA

Dissolution studies were conducted using an automated dissolution apparatus II with a rotation speed of 50 rpm (VanKel7000, Connecticut, USA). IPB pH 7.4 (150 mL) was used as the dissolution medium and maintained at 37 °C. The volume of the dissolution medium was justified from the LOQ of the analytical method. The dissolution study was performed on the IMC–CCC mixtures, IMC–CCC–LA, and IMC–cholesterol mixtures. The IMC–CCC mixtures (100 mg) were added to the dissolution apparatus II. At appropriate time intervals, 2 mL of the dissolution medium was withdrawn and immediately replaced with fresh medium. The dissolved IMC was analyzed using the HPLC assay.

In Vitro Permeation and Skin Experiments

In vitro skin permeation studies were performed using vertical diffusion Franz cells (Hanson Research Corporation,

California, USA) with an effective diffusion area of 1.77 cm^2 (28). The experiments were carried out using newborn pig skins. The skin, previously frozen at −20 °C, was pre-equilibrated overnight in IPB pH 7.4 at 25 °C before the experiments (29). A circular piece of this skin was sandwiched securely between the two halves of the cells with the stratum corneum side facing the donor compartment. The receiver compartment was filled with 12 mL of IPB pH 7.4 which was continuously stirred (400 rpm) and thermostated at 37 °C throughout the experiments (30). Approximately, 100 mg of the IMC–CCC mixture was applied to a new born pig skin and covered with Parafilm™ to prevent evaporation. At appropriate time intervals (0.5, 1, 2, 3, 4, 6, 8, 10, 12, 24 h), 1 mL samples were withdrawn from the receptor compartment and immediately replaced by an equal volume of fresh receptor solution. Samples were analyzed using the HPLC system. Following the skin permeation studies, after 24 h the diffusion cells were dismantled, the effective diffusion area was cut off and washed briefly in methanol. The skin was then homogenized in 5 mL of cold methanol for 10 min using a homogenizer (Ystral X10/25, Ballrechtar-Dottingen, Germany). The skin homogenate was centrifuged at 10,000×*g* for 10 min (Hettich Universal Zentrifuger 16R, Tuttlingen, Germany). The skin homogenate was filtered through a 0.22 μm cellulose acetate membrane to obtain a clear solution. The amount of IMC in the clear solution was then determined for IMC retained in the skin (31). The formulation that remained in the donor compartment after the permeation study was dissolved in methanol and adjusted to 25 mL in a volumetric flask. The formulation was sonicated until a clear solution was obtained and filtered through a cellulose acetate membrane (0.22 μm). Then the amount of IMC was analyzed by HPLC.

Stability Testing of the IMC–CCC Mixture

The short-term freeze–thaw stability of the samples was obtained over six freeze–thaw cycles, by thawing at 45 °C for 48 h and freezing at 4 °C for 48 h for each cycle, respectively (32). Sufficient samples (100 mg) were weighed and stored in the freezer. The IMC content from each storage period was compared with the initial concentration of the freshly prepared samples. The sample mixtures were evaluated for drug content, dissolution test and phase transition. The texture of the IMC–CCC mixture was observed with a PLM.

Analysis of Data

The IMC release kinetics were analyzed by zero-order (Eq. 1), first-order (Eq. 2), and the Higuchi's models (Eq. 3), respectively. They were applied to consider the amounts of the drug released from 30 min to 24 h.

$$Q_t = Q_0 + K_0 t \tag{1}$$

$$\ln Q_t = \ln Q_0 + K_f t \tag{2}$$

$$Q_t = K_H t^{1/2} \tag{3}$$

Q_t The cumulative amounts of drug release in time t
Q_0 The initial amount of drug in the preformed preparations
k_0 The release rate constants of zero order
k_f The release rate constants of first order
k_H The release rate constants of Higuchi's model

The paired t test was used to compare the percentage of drug released before and after the freeze–thaw cycles. A p value of less than 0.05 was considered to be statistically significant.

The cumulative amount of IMC released or permeated through the skin was calculated from the dissolution data and the *in vitro* permeation data, respectively, using the following equation 4:

$$Q_t = V_r C_t + \sum_{i-0}^{t-1} V_s C_i \tag{4}$$

C_t The drug concentration of the receptor fluid at each sampling time
C_i The drug concentration of the ith sample
V_r The volumes of the receptor fluid
V_s The sampling volume

In the permeation study, data were expressed as the cumulative drug permeation per unit of skin surface area Q_t/S (S=1.77 cm^2) (29). The steady-state fluxes (J_{SS} (0–24 h)) were calculated by linear regression interpolation of the experimental data at steady state (between 0 and 24 h, ΔT) as shown in Eq. 5.

$$J_{SS} = \Delta Qt/(\Delta TS) \tag{5}$$

The characterization data were expressed as the means of three experiments±SD. The skin permeation data were expressed as the means of at least four experiments±SD. One-way analysis of variance (ANOVA) and Tukey's multiple comparison tests were used to compare the fluxes of IMC from different preformed preparations.

RESULTS AND DISCUSSION

Solubility of Indomethacin in Isotonic Phosphate Buffer pH 7.4 at 37 °C

The concentration of IMC at 37 °C in isotonic phosphate buffer pH 7.4 at 24, 48, 72, 73, 74 and 75 h was 703.4±19.3, 785.7±9.6, 920.8±11.8, 921.2±7.5, 920.5±9.3 and 919.0±8.1 μg/mL, respectively (mean±SD, n=3). The concentration did not increase further after 72 h. From our study, the solubility of IMC was slightly higher than that of the reported value (800 μg/mL) (33). This is due to the reported value being obtained at a lower temperature and therefore it is anticipated to obtain a lower solubility. This value was used to justify the formulation loading in the dissolution tests of the IMC–CCC mixture, i.e., not limited by the IMC solubility.

Preparations of IMC–CCC, IMC–CCC–LA Mixtures

The uniformity of the IMC content of all IMC–CCC mixtures are as follows, 1 % IMC 95.4±0.02; 2 % IMC 95.9±0.02 and 5 % IMC 97.7±0.05 (mean±SD, n=3). The IMC–CCC–LA content was 99.2 %. The assay values are between 95.4–99.2 % (*w*/*w*). The IMC content was corrected to 100 % for further studies in all formulations.

FTIR Analysis of IMC–CCC, IMC–CCC–LA Mixture

From the FTIR spectrum of CCC (Fig. 1), there are three main peaks for methylene, carbonate ester and carbonyl group. The methylene group shows two distinct bands of C–H stretching located at 2,918 and 2,848 cm^{-1}. The carbonate ester of CCC appears at 1,467 and 1,289 cm^{-1} corresponding to the O–C–O stretching mode. The carbonyl carbonate (C=O) stretching was at 1,743 cm^{-1} (25).

The FTIR spectra of CCC, pure IMC, IMC–CCC and IMC–CCC–LA mixtures with different drug contents (1, 2, 5 % IMC) are shown in Fig. 1. The pure CCC gives a carbonyl stretching at 1,743 cm^{-1} whereas IMC appears at 1,717 and 1,691 cm^{-1}. The higher the content of IMC in the IMC–CCC mixture, the stronger the appearance of the peaks for the C=O stretching. These results indicated that there may be some interactions between IMC and CCC. This was because the wavelength of the carbonyl group of CCC was shifted 17 cm^{-1} from 1,736 to 1,719 cm^{-1}, whereas there was no change observed in the finger print region of the FTIR spectra.

DSC Analysis of IMC–CCC, IMC–CCC–LA Mixture

In the case of pure IMC or CCC, endothermic peaks were observed at 140 and 71 °C, respectively. Both compounds were crystallized from chloroform. The IMC at concentrations of 1, 2, and 5 % (*w*/*w*) were completely incorporated into CCC. However, the IMC–CCC at the higher ratio (10 %) did not produce a homogeneous mixture (data not shown).

At concentrations of 1, 2 and 5 % IMC (*w*/*w*) in the formulation, the mixtures showed only one endothermic peak of CCC at 71 °C. This result indicated that the IMC can be completely incorporated into the CCC. Similarly, 5 % IMC was also completely incorporated into the CCC–LA mixtures as the thermogram shows no endothermic peak over 20–200 °C.

When liquid crystals are developed for transdermal application, it is necessary to consider that the transition temperature of the formulation should be close to the skin temperature (32 °C). At the skin temperature, IMC should be released completely from the liquid crystalline structure of the IMC–CCC mixture. However, the thermogram of the IMC–CCC mixture showed that the endothermic peak at

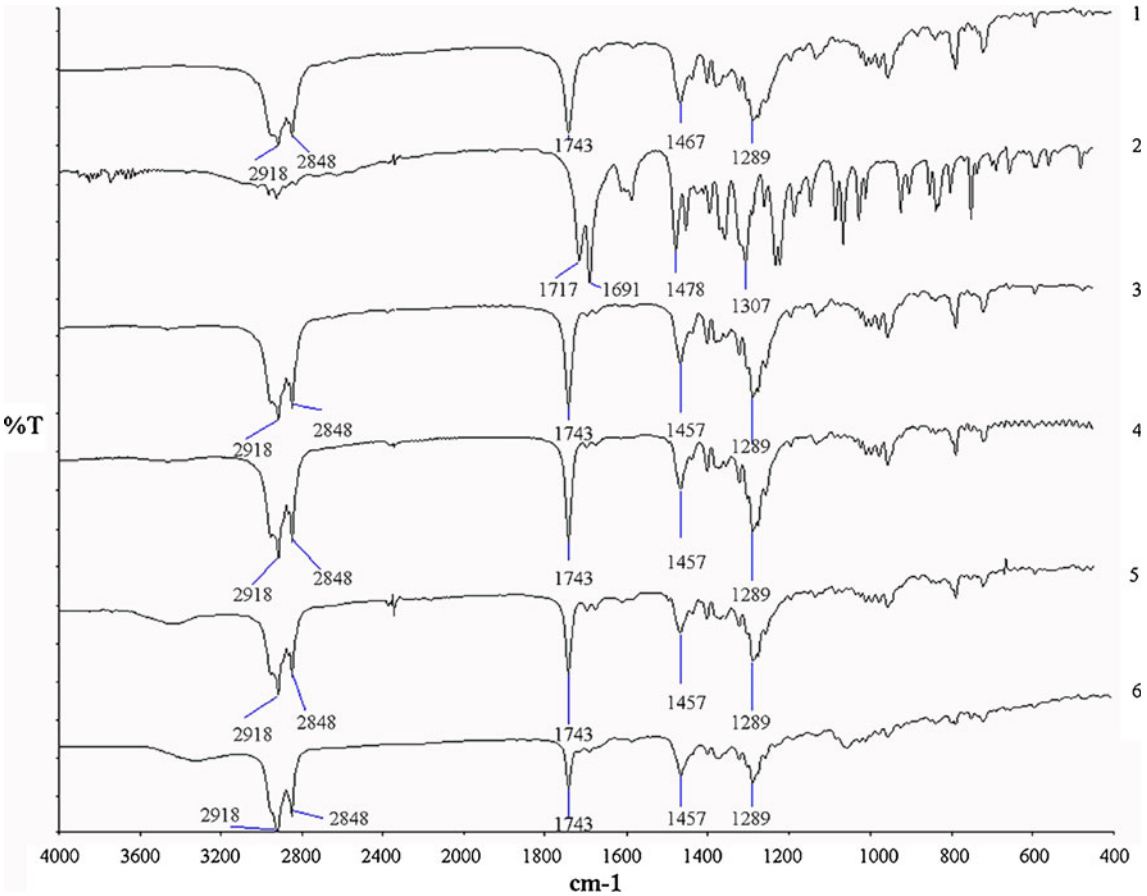

Fig. 1. FTIR spectra of CCC (*1*), pure indomethacin (*2*) and indomethacin–CCC (IMC–CCC) mixtures at 1 % IMC (*3*), 2 % IMC (*4*), 5 % IMC (*5*), and 5 % IMC in CCC–LA (*6*)

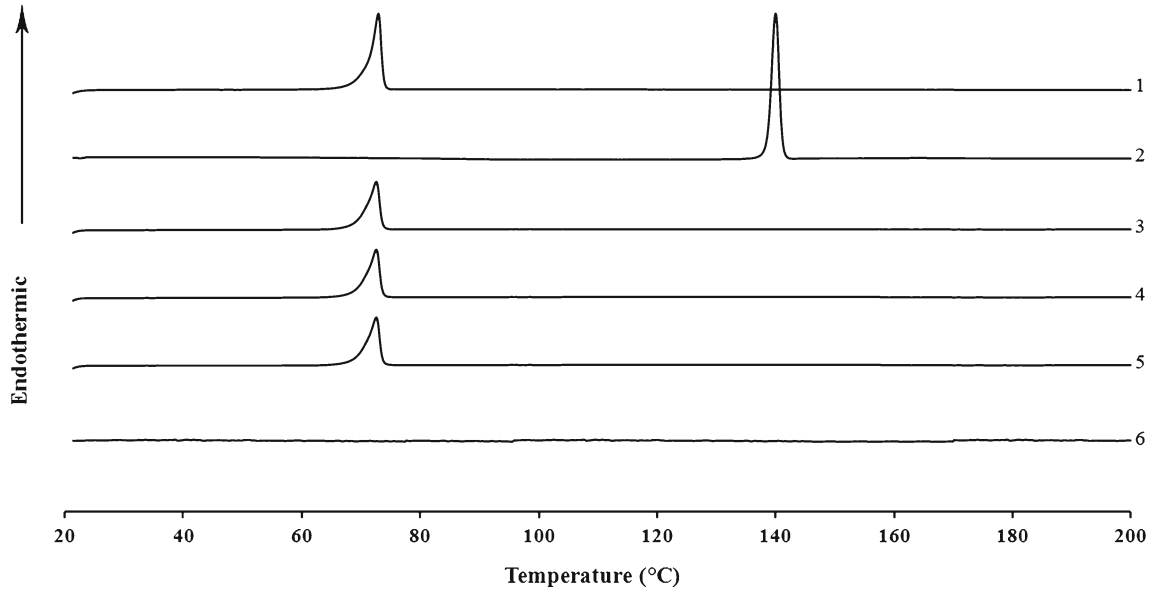

Fig. 2. DSC thermograms of CCC (*1*), pure indomethacin (*2*) and indomethacin-CCC mixture (IMC–CCC) at 1 %IMC (*3*), 2 % IMC (*4*), 5 % IMC (*5*) and 5 % IMC in CCC–LA (*6*)

71 °C was far from 32 °C. Therefore, it is important to decrease the phase transition temperature by adding other components (e.g., lauryl alcohol) into the liquid crystalline system to bring down the phase transition temperature closer to 32 °C. In this case, we found that the transition temperature of IMC–CCC–LA disappeared over 20–200 °C (Fig. 2). It meant the formulation is in an amorphous state. It was soft semi-solid and easy to apply to the skin.

PLM of the IMC–CCC, IMC–CCC–LA Mixture

The birefringence of CCC was observed from the macroscopic structure of the liquid crystalline phases. The results from PLM showed that the texture of the CCC did not rearrange to a spherulite. It rather shows the maltese cross of CCC at 25 °C before being heated (Fig. 3a). Figure 3b shows spherulites with different sizes of CCC at 32 °C. Upon heating, the crystals melted at 71 °C. After cooling down to 25 °C, CCC rearranged itself to an orderly spherulite (Fig. 3c). In this case, the spherulites are more uniform in size than those observed at 32 °C. During heating, the texture of the CCC showed the phase transition from a solid crystal (maltese cross) to an isotropic liquid and an isotropic liquid back to a solid crystal (spherulite) on cooling. The results from this study indicated that the molecular arrangement of CCC is time and temperature dependent. It is postulated that more IMC could be released from CCC at 32 °C than at 25 °C. This conclusion derives from a temperature difference of 7° causing a lower order of liquid crystal.

From the PLM results, a poor birefringence of the IMC–CCC mixture was obtained during the heating process and a liquid state was observed at temperatures above 73 °C. During the cooling down process, the nematic phase of the IMC–

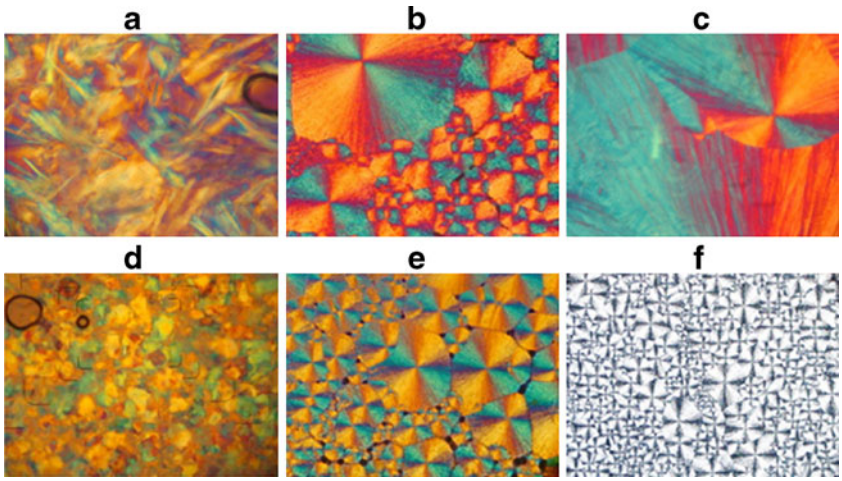

Fig. 3. Cholesteryl cetyl carbonate (CCC) from polarized light microscope at 25 °C (**a**), after recrystallization from molten state at 32 °C (**b**) and at 25 °C (**c**), 5 % indomethacin-CCC (IMC–CCC) mixture at 25 °C (**d**) and after recrystallization from molten state (**e**) and IMC–CCC–LA (**f**) (×400)

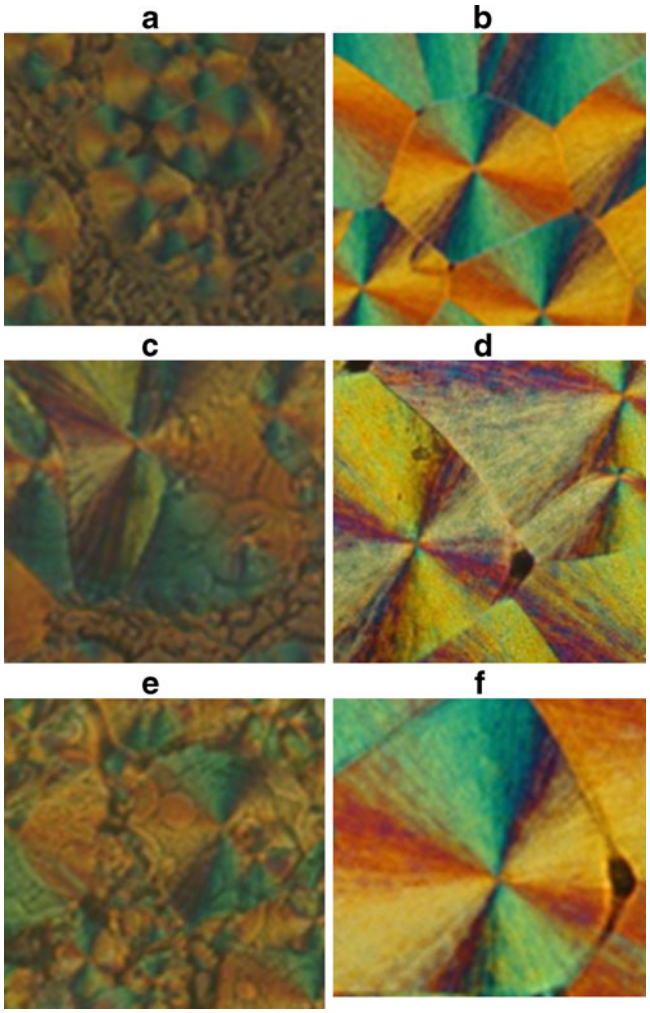

Fig. 4. Texture of 1 %IMC (**a**), 2 %IMC (**c**), and 5 % IMC (**e**) in CCC from polarized light microscope at 25 °C and after recrystallization from molten state (**b**, **d**, **f**) of the same preformed in respective order (×400)

CCC mixtures occurred at temperature of between 71 and 55 °C. Whereas, the nematic–smectic phase transition temperature was 54 °C and the smectic–solid phase transition temperature occurred at 54–42 °C. The results revealed that the incorporation of IMC into CCC did not alter the three phase transition temperatures during the cooling down process. The birefringence of IMC–CCC remained unchanged as detected by PLM when compared to that of pure CCC. It is important to note that no spherulites were observed in the IMC–CCC mixture before heating (Fig. 3d), whereas the spherulite texture was observed after the mixture was cooled down to 25 °C (Fig. 3e). This also contributed to the IMC–CCC mixtures becoming rearranged to more ordered crystals. When LA was incorporated as a third component in the formulation, the texture changed significantly from hard to soft. PLM revealed spherulite and fan shapes of the mixture but the image did not give a bright color (Fig. 3f).

All IMC–CCC mixtures at 32 °C exhibited spherulite textures (Fig. 4) similar to those observed at 25 °C. However, the higher temperatures resulted in less ordering of the molecules when compared to that at the lower temperatures. Thus, the birefringence of the IMC–CCC mixture at 32 °C was slightly different from that at 25 °C. Moreover, there were no differences observed with the different concentrations of IMC (1, 2, and 5 %) mixed into the CCC.

Dissolution Test of IMC–CCC, IMC–CCC–LA Mixture

The dissolution profiles of the IMC–CCC, IMC–CCC–LA mixtures are illustrated in Fig. 5. For all mixtures, the drug was gradually released with time over a 24-h period. The IMC–CCC mixtures regulated the release of IMC. In the case of 1 % IMC in cholesterol, the drug was immediately released within 30 min. The release of IMC incorporated into cholesterol was found to reach its maximum within 3 h, whereas the release of IMC from the IMC–CCC mixtures of 1, 2, and 5 % IMC was delayed for up to at least 24 h. It meant that cholesterol enhanced the release of IMC rather than retarded its release. This is related to its emulsifying property. The dissolution and permeation of 5 %IMC in the CCC–LA mixture is shown in Fig. 6. The release of 5 %IMC in CCC–LA was very close to 1 %IMC in CCC, it meant that the addition of the fatty alcohol controlled the release of IMC.

The data obtained from the release studies were evaluated kinetically, and fitted to three different kinetic models: zero

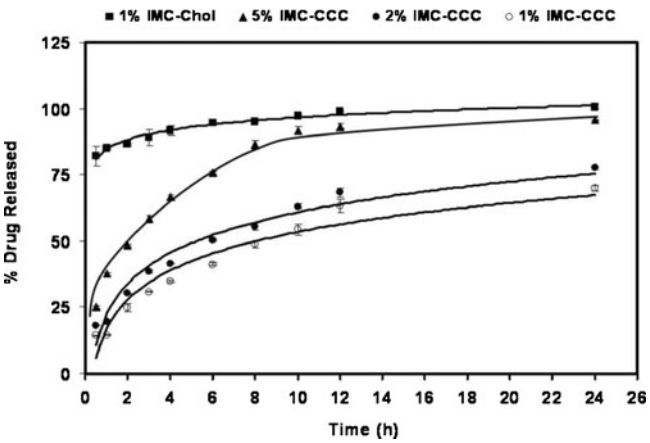

Fig. 5. The dissolution profiles of indomethacin-CCC (IMC–CCC) mixtures at 1 % indomethacin (*open circle*), 2 % indomethacin (*filled circle*) and 5 % indomethacin (*filled upright triangle*), and 1 %indomethacin in cholesterol (IMC-Chol) (*filled square*) (mean±SD, $n=3$)

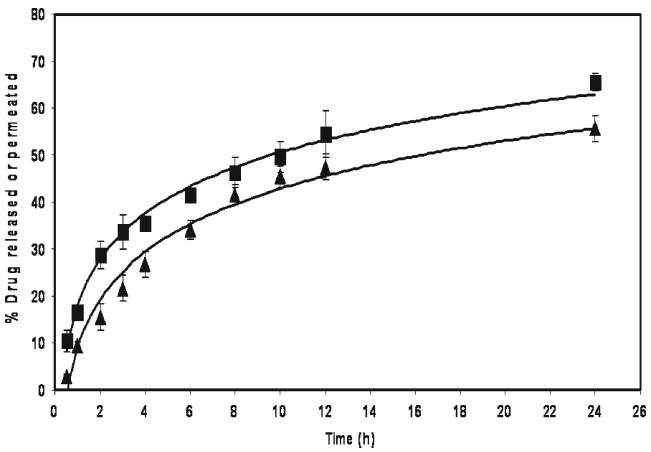

Fig. 6. The dissolution profiles (*filled square*) and permeability profile (*filled upright triangle*) of 5 % indomethacin in CCC–LA mixtures (mean±SD, $n=3$)

Table I. Release Kinetic Parameters of Indomethacin (IMC) Release from Preformed Preparations (mean±SD, n=3)

Kinetic Model		1 % IMC–CCC	2 % IMC–CCC	5 % IMC–CCC	5 %IMC–CCC–LA
Zero order	R^2	0.997	0.984	0.936	0.805
	k_0 (μg/mL h)	33.98±1.75	69.94±3.43	199.03±2.66	14.98±1.8
First order	R^2	0.978	0.981	0.996	0.958
	k_1 (h^{-1})	0.06±0.00	0.07±0.00	0.22±0.01	0.47±0.02
Higuchi	R^2	0.994	0.997	0.993	0.968
	k (μg/mL $h^{1/2}$)	166.61±7.6	346.04±16.68	1387.33±45.65	97.25±7.67

k_0, k_1, and k are release rate constant of zero-order, first-order, and Higuchi models, respectively

order, first order, and Higuchi. The release rate constants of each model are summarized in Table I.

The correlation coefficient of the linear regression was greater than 0.93 in all models except that in 5 %IMC–CCC–LA which was about 0.81. In all ratios, the Higuchi model best fitted the release of IMC from the IMC–CCC mixture, whereas the first- and zero-order models were less justified. So based on those three concentrations, the release of IMC from the IMC–CCC mixtures complied with the Higuchi kinetic model. From the Higuchi model, the release rate constants of 1, 2, and 5 % IMC–CCC mixtures were 166.6, 346.0, and 1387.3 μg mL^{-1} $h^{-1/2}$, respectively. Whereas 5 % IMC–CCC–LA release rate constant was 97.3 μg mL^{-1} $h^{-1/2}$. CCC may work as a matrix in the mixture (34). As the concentrations of IMC increased from 1 to 5 %, the release rate constants in CCC were significantly increased (p<0.05).

In Vitro Skin Permeation

The *in vitro* skin permeation tests of various IMC–CCC mixtures were evaluated using a modified Franz diffusion cell. The amount of IMC that penetrated through the skin into the receptor fluid was too small to be detected during the 24 h of experiment. However, we observed a peak of IMC in the chromatogram but it was too small to be quantitated (LOQ <0.83 μg/mL). The LOQ for IMC in IPB, methanol and supernatant were 0.83, 1.73, and 1.00 μg/mL, respectively.

However, when LA was incorporated into the IMC–CCC mixture it was found that the permeation of IMC across the skin was significantly increased to a level of 45 % in 24 h (Fig. 6). The amount of IMC remaining in the donor phase was decreased significantly (35–40 %) in accordance with the permeate IMC. There was some amount of IMC (2 %) that retained in the skin.

The retained IMC in the skin at 24 h in the presence of 1, 2, and 5 % IMC, 5% IMC-CCC-LA and a 1 % IMC–cholesterol mixture was 5.17, 2.61, 1.05, 2.20, and 2.40 %, respectively (Fig. 7). It is likely that 1 % IMC–CCC exhibited the highest percentage of IMC retained in the newborn pig skin than the other formulations. However, the calculation revealed that those three formulations containing CCC gave approximately the same amount of IMC retained in the skin to indicate that the skin became saturated with IMC. In practice, IMC saturation may not occur since IMC is taken into the blood circulation from the dermis layer. It is important to point out that CCC enhanced the retained IMC in the pig skin better than cholesterol (p<0.05).

Only a small percentage of the IMC was retained in the newborn pig skin compartment. However, the amount of drug that remained in the donor compartment for the 1, 2, and 5 % IMC–CCC and the IMC–cholesterol mixture were found to be 88.27±1.3, 95.97±2.0, 97.85±2.1, and 95.98±1.6 %, respectively. In such case, the amount of IMC in the donor phase may act as a drug reservoir to release and permeate across the stratum corneum when the system was not at equilibrium.

Following the skin permeation studies, the newborn pig skin was extracted by deuterated chloroform ($CDCl_3$) and the CCC content was monitored by ^{13}C-NMR. This showed all the chemical shifts of CCC. The chemical shift at 154.68 ppm of the carbonyl carbonate ester was especially clearly shown in the spectrum. It indicated that CCC penetrated into the skin and was retained within the skin. Thus, it is likely that CCC was transported together with IMC. The present formulation

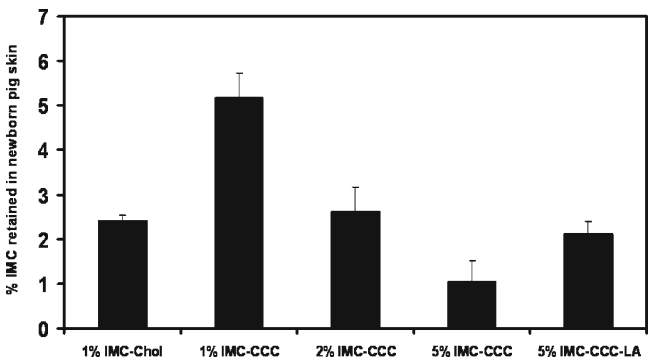

Fig. 7. Percentage of indomethacin (IMC) retained in excised newborn pig skin at 24 h after application of 1% IMC in cholesterol (1% IMC-Chol), 1, 2, 5% IMC in CCC and 5%IMC-CCC-LA (mean ± SD, n=4)

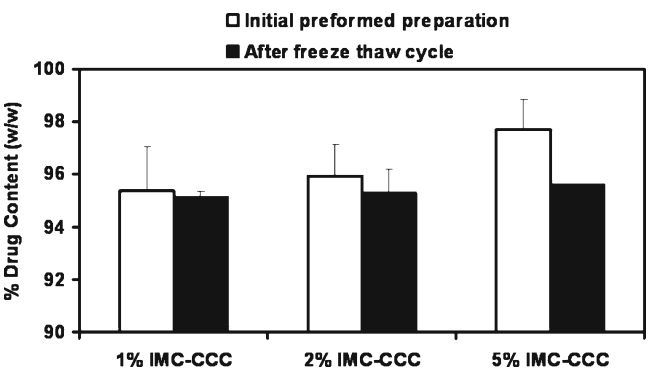

Fig. 8. The indomethacin (IMC) content in CCC at initial preformed mixtures of 1, 2, 5% IMC-CCC (*white rectangle*) and after freeze thaw cycle (*dark rectangle*) (mean ± SD, n=3)

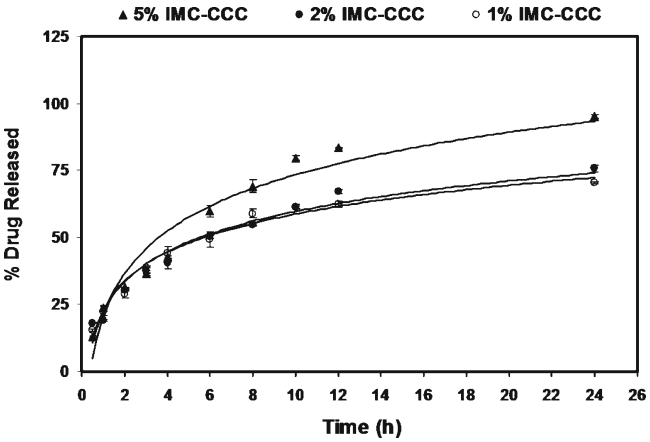

Fig. 9. The dissolution profiles of indomethacin-CCC (IMC-CCC) at 1 (*open circle*), 2 (*filled circle*) and 5% (*filled upright triangle*) after freeze thaw cycle (mean ± SD, n=3)

of IMC–CCC–LA is suitable for a transdermal preparation. The IMC–CCC–LA formulation should be further optimized for drug loading and for suitable ratios of CCC to LA.

Stability Testing of the IMC–CCC Mixture

The uniformity of the drug content of the initial IMC–CCC preparation and after the freeze–thaw cycle is shown in Fig. 8. All the initial preparations showed a slight but not significant higher drug content than after the freeze–thaw cycle (paired *t* test, $p>0.05$). This indicated that although freeze–thawing reduced the content slightly it was insignificant and all three sample preparations were stable at room temperature

FTIR Analysis of the IMC–CCC Mixture After a Freeze–Thaw Cycle

All preformed preparations showed a spectrum that was not different from its initial value. At the higher percentage of IMC, a sharper peak of the C=O stretching of IMC at 1,716 and 1,692 cm^{-1} was obtained. Based on these results, it can be claimed that the chemical properties of the IMC–CCC mixtures were not changed after the freeze–thaw cycle. At the higher concentration of IMC (5 % IMC–CCC) in the mixture, the peak characteristics of IMC were clearly observed. It clearly indicates that IMC was stable in the mixtures.

DSC Analysis of the IMC–CCC Mixture After a Freeze–Thaw Cycle

All the IMC–CCC mixtures after the freeze–thaw had an endothermic peak at 73 °C on the heating run. Upon cooling from its isotropic liquid phase, the IMC–CCC mixtures had three exothermic peaks at 65, 47 and 40 °C which had shifted to a lower temperature than that observed with the IMC–CCC mixtures before the freeze–thaw cycle by about 2–8°. It is possible that the IMC incorporated into CCC may affect the arrangement of CCC resulting in a lower phase transition temperature. However, it is most likely that the chemical structure of CCC remained unchanged but physically it did change slightly as the phase transition temperature decreased.

PLM of the IMC–CCC Mixtures After a Freeze–Thaw Cycle

The birefringence of the IMC–CCC mixtures was observed after the freeze–thaw cycle. Upon heating, the crystals melted at 72 °C. After cooling down to 25 °C, CCC rearranged itself to an orderly spherulite. The birefringence of the IMC–CCC mixtures was transformed to a more orderly structure after being cooled down as compared to that of the initial preformed preparations. It is expected that the IMC–CCC molecules rearrange themselves to become perfect uniform spherulites. However, any interaction between IMC and CCC molecules needs analysis by a more advanced technique such as single crystal X-ray crystallography to explain any changes at the molecular level.

Dissolution Test of the IMC–CCC Mixtures After a Freeze–Thaw Cycle

Figure 9 shows the dissolution profiles of the IMC–CCC mixtures after a freeze–thaw cycle. The percentage release of IMC in all preformed preparations did not change (Figs. 5 and 8). However, for the 5 % IMC–CCC mixture, the release was decreased. It is possible that at a 5 % IMC loading the freeze–thaw cycle changed the physicochemical properties of IMC–CCC system resulting in a decrease of the drug release.

Table II summarizes the kinetic data obtained from the Higuchi plots of each dissolution profile after the freeze–thaw cycle of the preformed preparations compared with the initial preparations. The linear regression correlation coefficient obtained was greater than 0.97. The release rate constants of the IMC–CCC mixtures before and after the freeze–thaw cycles were not significantly different ($p>0.05$). For all three preformed IMC–CCC mixtures (1, 2, and 5 % IMC), the release rate constants decreased from the initial but not significantly. The difference was most pronounced in the 5 % IMC–CCC mixture. This may result from the recrystallization of CCC during the freeze–thaw cycle. The crystal structure of CCC may affect the release of IMC. However, this evidence has to be proven in longer term stability studies of the IMC–CCC mixtures.

Table II. Higuchi Release Rate Constant of Indomethacin-CCC (IMC–CCC) Mixtures After Freeze–Thaw Cycle Compared with Initial Preformed Preparations (mean±SD, $n=3$)

	Release rate constant ($\mu g/mL \cdot h^{1/2}$)			Correlation coefficient of release profile (R^2)	
Preformed preparations	Initial	After freeze–thaw cycle	*p* value	Initial	After freeze–thaw cycle
1 % IMC–CCC	166.61±7.6	152.33±1.94	>0.05	0.994	0.970
2 % IMC–CCC	346.04±16.68	334.50±5.60	>0.05	0.997	0.995
5 % IMC–CCC	1387.33±45.65	1106.00±34.04	>0.05	0.993	0.972

From this study, it can be seen that the IMC can be incorporated into CCC at low concentrations (low loading capacity). The IMC–CCC system can also release the drug in a controlled manner. When LA was incorporated into the IMC–CCC mixture it enhanced the drug permeation across the skin. This system could operate as a transdermal, semi-solid dosage form because IMC is able to permeate across the barrier of the skin. At this stage, this system is suitable for transdermal formulation. However, further improvement can be made to the drug loading.

CONCLUSIONS

In this study, IMC was developed in a transdermal dosage form by incorporation CCC together with LA. CCC by itself was not a promising carrier system for transdermal drug delivery. However, the addition of LA decreased the transition temperature closer to that of the skin temperature. This also enhances the permeation of IMC across the skin. Other issues that can be examined in the future are the interactions between IMC and CCC at a molecular level using single crystal X-ray crystallography. This would require the crystallization of pure IMC, pure CCC and co-crystallization of the IMC–CCC mixture.

REFERENCES

1. Shen TY. The discovery of indomethacin and the proliferation of NSAIDs. Seminars in Arthritis and Rheumatism. 1982;12:89–93.
2. Kulmacz RJ. Topography of prostaglandin H synthase. Antiinflammatory agents and the protease-sensitive arginine 253 region. J Biol Chem. 1989;264:14136–44.
3. Fang WF, Broughton A, Jacobson ED. Indomethacin induced intestinal inflammation. Am J Dig Dis. 1977;22:749–60.
4. Yamada T, Deitch E, Specian RD, Perry MA, Sartor RB, Grisham MB. Mechanisms of acute and chronic intestinal inflammation induced by indomethacin. Inflammation. 1993;17:641–62.
5. The Merck Index. 12 ed. Whitehouse NJ: Merck &Co., Inc.; 1996.
6. Surya Prakash BNG, Hari Narayana Moorthy NS. Synthesis and physicochemical characterization of mutual prodrug of indomethacin. Trends Applied Sci Res. 2007;2:165–9.
7. Jambhekar S, Casella R, Mahera T. The physicochemical characteristics and bioavailability of indomethacin from β-cyclodextrin, hydroxyethyl-β-cyclodextrin and hydroxypropyl-β-cyclodextrin complexes. Int J Pharm. 2004;270:149–66.
8. Cai X, Yang L, Zhang LM, Wu Q. Synthesis and anaerobic biodegradation of indomethacin-conjugated cellulose ethers used for colon-specific drug delivery. Bioresour Technol. 2009;100:4164–70.
9. Jona JA, Dittert LW, Crooks PA, Milosovich SM, Hussain AA. Design of novel prodrugs for the enhancement of the transdermal penetration of indomethacin. Int J Pharm. 1995;123:127–36.
10. Spireas S, Sadu S. Enhancement of prednisolone dissolution properties using liquid solid compacts. Int J Pharm. 1998;166:177–88.
11. Loukas YL, Vraka V, Gregoriadis G. Drugs in cyclodextrins, in liposomes: a novel approach to the chemical stability of drugs sensitive to hydrolysis. Int J Pharm. 1998;162:137–42.
12. Loukas YL, Gregoriadis G. Drugs, in cyclodextrins, in liposomes: a novel approach for the reduction of drug leakage from liposomes. Proceedings of the Twenty fourth International Symposium on Controlled Release of Bioactive Materials. Stockholm, Sweden, June 15–19, 1997.
13. Chandrasekaran S, Al-Ghananeem AM, Riggs RM, Crooks PA. Synthesis and stability of two indomethacin prodrugs. Bioorg Med Chem Lett. 2006;16:1874–9.
14. Pohlmann AR, Weiss V, Mertins O, Pesce da Silveira N, Guterres SS. Spray-dried indomethacin-loaded polyester nanocapsules and nanospheres: development, stability evaluation and nanostructure models. Eur J Pharm Sci. 2002;16:305–12.
15. Fitzpatrick D, Corish J. Release characteristics of anionic drug compounds from liquid crystalline gels I: passive release across non-rate-limiting membranes. Int J Pharm. 2005;301:226–36.
16. Trotta M. Influence of phase transformation on indomethacin release from microemulsions. J Control Release. 1999;60:399–405.
17. Fujii M, Shiozawa K, Watanabe Y, Matsumoto M. Effect of phosphatidylcholine on skin permeation of indomethacin from gel prepared with liquid paraffin and hydrogenated phospholipid. Int J Pharm. 2001;222:57–64.
18. Suzuki T, Yoda K, Iwai H, Fukuda K, Hotta H. Multiphase emulsions by liquid crystal emulsification and their application. Studies in Surface Science and Catalysis. 2001;132:1025–30.
19. Muller-Goymann CC. Physicochemical characterization of colloidal drug delivery systems such as reverse micelles, vesicles, liquid crystals and nanoparticles for topical administration. Eur J Pharm Biopharm. 2004;58:343–56.
20. Lee J, Kellaway IW. *In vitro* peptide release from liquid crystalline buccal delivery systems. Int J Pharm. 2000;195:29–33.
21. Lin SY, Ho CJ, Li MJ. Precision and reproducibility of temperature response of a thermo-responsive membrane embedded by binary liquid crystals for drug delivery. J Control Release. 2001;73:293–301.
22. Makai M, Csányi E, Németh Zs, Pálinkás J, Erős I. Structure and drug release of lamellar liquid crystals containing glycerol. Int J Pharm. 2003;256:95–107.
23. Chuealee R, Wiedmann TS, Suedee R, Srichana T. Interaction of amphotericin B with cholesteryl palmityl carbonate ester. J Pharm Sci. 2010;99:4593–602.
24. Chuealee R, Wiedmann TS, Srichana T. Physicochemical properties and antifungal activity of amphotericin B incorporated in cholesteryl carbonate esters. J Pharm Sci. 2011;100:1727–35.
25. Chuealee R, Wiedmann TS, Srichana T. Thermotropic behavior of sodium cholesteryl carbonate. J Mater Res. 2009;24:156–63.
26. Fischer P, Eugster A, Windhab EJ, Schuleit M. Predictive stress tests to study the influence of processing procedures on long term stability of supersaturated pharmaceutical o/w creams. Int J Pharm. 2007;339:189–96.
27. Bagheri M, Rad RZ. Synthesis and characterization of thermotropic liquid crystalline polyesters with biphenyl unit in the main chain. React Funct Polym. 2008;68:613–22.
28. Siewert M, Dressman J, Brown CK, Shah VP. FIP/AAPS guidelines to dissolution/*in vitro* release testing of novel/special dosage form. AAPS Pharm. Sci. Tech. 2003;4:Article 7.
29. Songkro S, Purwo Y, Becket G, Rades T. Investigation of newborn pig skin as an *in vitro* animal model for transdermal drug delivery. STP Pharm Sci. 2003;13:133–9.
30. Michniak BB, Player MR, Chapman JM, Sowell JW. *In vitro* evaluation of a series of azone analogs as dermal penetration enhancers. Int J Pharm. 1993;91:85–93.
31. Yoo J, Shanmugam S, Song CK, Kim DD, Choi HG, Yong CS, *et al*. Skin penetration and retention of L-ascorbic acid 2-phosphate using multilamellar vesicles. Arch Pharm Res. 2008;31:1652–8.
32. Shafiq-un-Nabi S, Shakeel F, Talegaonkar S, Ali J, Baboota S, Ahuja A, et al. Formulation development and optimization using nanoemulsion technique: a technical note. AAPS Pharm. Sci. Tech. 2007;8: Article 28.
33. O'Brien M, McCauley J, Cohen E. Analytical Profiles of Drug Substances. In: Florey K, editor. Indomethacin. San Diego: Academic Press Inc; 1984. p. 211–38.
34. Boyd BJ, Khoo SM, Whittaker DV, Davey G, Porter CJ. A lipid-based liquid crystalline matrix that provides sustained release and enhanced oral bioavailability for a model poorly water soluble drug in rats. Int J Pharm. 2007;340:52–60.